AN EXPERIMENTAL <u>IN</u> <u>SITU</u> DENSITOMETER

by

Howard W. Kuenzler

B.E.E., University of Florida

(1964)

Submitted in Partial Fulfillment

of the Requirements for the

Degree of Master of Science

in Oceanography

at the

Massachusetts Institute of Technology

August, 1968

Signature of Author _____
              Department of Geology and Geophysics, August 19, 1968

Certified by _____
                                                    Thesis Supervisor

Accepted by _____
                              Chairman, Departmental Committee
                                         on Graduate Students

AN EXPERIMENTAL <u>IN</u> <u>SITU</u> DENSITOMETER

by

Howard W. Kuenzler

Submitted to the Department of Geology and Geophysics

on 19 August 1968

in partial fulfillment of the requirement for

the degree of

Master of Science in Oceanography

Abstract

A new prototype transducer capable of making direct measurements of fluid density <u>in</u> <u>situ</u> has been developed. The theory of design, the method of construction, and the performance in laboratory tests are discussed in view of its possible application as an oceanographic tool for precise measurement of seawater density. Present sensitivity is within an order of magnitude of the capabilities of indirect techniques currently being used for seawater. Suggestions are made for improving the precision, and indications are given that the device has potential as a sea-going oceanographic instrument.

Thesis Supervisor: Eric Mollo-Christensen
Title: Professor of Meteorology

Table of Contents

List of Figures

List of Tables

INTRODUCTION

Many techniques have been proposed and developed to make measurements of fluid density. Some give direct measures while others infer density from other measurable quantities. Their precision and accuracy vary widely.

For the oceanographer who needs to detect small yet very important differences in density in the ocean, only one technique has gained wide acceptance as being both practical and having sufficient sensitivity. The technique is an indirect one, allowing density to be calculated from measurements of temperature, salinity, and pressure. Confidence has been placed in it because of the apparent consistency of the empirical relationships derived from chemical analyses on water samples from different oceanic regions during the past seventy years.

It has been a fortunate situation for those whose interest has been in the dynamics of ocean circulation that water found in widely separated basins across the globe has had a set of characteristics sufficiently similar to allow a single empirical relationship developed originally by Knudsen in 1902 (Carritt & Carpenter, 1958) to be used for all. There are many places, however, where this single relationship cannot be trusted to the accuracy implied because the assumptions on which the relationship is based are not strictly valid. Examples are to be found in coastal regions highly influenced by continental runoff, in biologically active areas containing significant amounts of organic material and detritus, in water where silt and suspended material are present, and in any region where the relative proportions of constituents differ significantly from the waters that produced the empirical relationship.

The feeling that if density is required then density should be measured directly has prompted this author to develop an instrument that can make continuous in-situ measurements of fluid density to an accuracy commensurate with oceanographic requirements. The result has been a prototype instrument which, with only minor modifications, can be converted into a sea-going device. Other changes which will improve its sensitivity and accuracy have also become clear during the development.

Although this device is significantly different in principle from previous density transducers, the author wishes to recognize Dr. W. S. Richardson for originally bringing to his attention the possibility of a density-to-frequency transducer by his suggestion for a vibrating rod densitometer (Richardson, 1958).

THEORY OF OPERATION

A. General Scheme

The transducer head is a four-vaned stainless steel unit having a bisecting web for rigidity. (See Figure I.) It is mounted between two cylindrical torsion bars which provide a torsional restoring force. Immediately above the head a coil of fine magnet wire is wound so that its plane is parallel to the axis of the torsion bars. (See Figure I.) The entire assembly is then mounted rigidly by its ends between the shaped pole pieces of a large magnetron magnet such that the plane of the coil lies parallel to the magnetic field, in a fashion similar to a galvanometer movement. A small current passed through the coil at the torsional resonant frequency provides the torque necessary to excite a periodic small amplitude angular displacement of the transducer head. The value of the resonant frequency depends in a simple way upon the stiffness of the torsion bars and the density of the fluid into which the head is immersed. A four-arm active strain gage bridge mounted on one torsion bar at its base senses the angular displacement and provides an electrical signal for positive feedback to sustain the oscillations. An accurate measurement of frequency is converted into an accurate measure of fluid density by calibration. The relative ease with which precise frequency measurement can be made with modern preset counters makes this kind of transducer most attractive.

B. The Transducer Head

This four-vaned unit forces into motion a small volume of fluid in its immediate vicinity. When in torsional vibration, each vane resembles a dipole acoustic source. Its four vanes acting together in close proximity then approximate an octupole radiator of acoustic energy. The

intensity in the radiation field decreases inversely as the 9th power of the distance from the head, making this design highly inefficient as an acoustic source. It is just this characteristic, however, that makes the design highly desirable as a density transducer. It insures that the volume of fluid influenced by transducer motions is of the order of the dimensions of the head, and therefore insures that the transducer responds only to changes in the local fluid density. Because the decay of field intensity with distance is caused by phase interference rather than by spherical spreading or absorption phenomena, the effects of small changes in acoustic parameters on the size of the virtual mass can be safely ignored. Comparisons of the resonant frequency in water with that in air have shown that the effective diameter of the virtual mass of fluid entrained is only 70% of the diameter of the transducer head itself.

Because the acceleration of every portion of the transducer head is sufficiently low, there is no danger of cavitation within the fluid.

C. Torsional Oscillations

When a mechanical system such as the one described having a transducer with moment of inertia I and torsion bars with spring constant k is excited by a sinusoidal torque of amplitude $\hat{\tau}$ and radian frequency ω, its angular displacement θ is given by the differential equation,

$$I \frac{d^2\theta}{dt^2} + \mu \frac{d\theta}{dt} + k\theta = \hat{\tau}e^{i\omega t} \tag{1}$$

where t is time and μ is the damping coefficient. The complex amplitude $\hat{\theta}(\omega)$ is found to be,

$$\hat{\theta}(\omega) = \hat{\tau} \frac{(k - I\omega^2) - i\mu\omega}{(k - I\omega^2)^2 + (\mu\omega)^2} \quad . \tag{2}$$

If the frequency is adjusted so that the angular response lags the applied

torque by 90°, then the real part of (2) must be zero, so that,

$$\omega = (\frac{k}{I})^{1/2} \equiv \omega_r \quad .$$ (3)

Equation (3) defines the resonant frequency. It should be noted that when

torsional oscillations are sustained such that θ lags τ by 90°, the reso-

nant frequency is not dependent upon μ. This insures that ω_r will not be

a function of dissipation in the system. In terms of its electrical analog,

ω_r is called the unity power factor frequency because at this frequency

current and applied voltage are in phase.

The period P_r is given by,

$$P_r = (\frac{4\pi^2}{k})^{1/2} I^{1/2} \quad .$$ (4)

When the transducer is placed into a fluid, its effective moment of inertia

is increased because of the virtual mass of entrained fluid. The moment

of inertia of the virtual mass is directly proportional to its density ρ,

so that,

$$P_r = (\frac{4\pi^2}{k})^{1/2} (I + C\rho)^{1/2} \quad \text{(seconds)}$$ (5)

where C is a geometrical factor equal to the volume moment of inertia of

the accelerated fluid. Combining the constants and letting $K_1 = \frac{4\pi^2}{k} I$ and

$K_2 = \frac{4\pi^2}{k} C$, equation (5) becomes,

$$P_r = (K_1 + K_2\rho)^{1/2} \quad \text{(seconds)} \quad .$$ (6)

The first constant accounts for the apparent density of the transducer

head itself while the second constant relates to the virtual volume of

fluid. Both are determined experimentally. When equation (6) is plotted

on a log-log graph, it is a straight line. This provides a good check for experimental data.

The magnitude of $\hat{\theta}$ (ω) is obtained from equation (2) and is given by,

$$| \hat{\theta} (\omega) | = | \hat{\tau} \frac{1}{(k - I\omega^2) + i\mu\omega} |$$

$$= \frac{\hat{\tau}}{I} [\frac{1}{(\omega_r^2 - \omega^2)^2 + (\frac{\mu\omega}{I})^2}]^{1/2} \qquad (7)$$

At the half-power frequency ω_1 on the frequency response curve, the amplitude of the response is $\frac{1}{\sqrt{2}}$ times the amplitude at $\omega = \omega_r$, so that

$$\frac{\hat{\tau}}{I} [\frac{1}{(\omega_r^2 - \omega_1^2)^2 + (\frac{\mu\omega_1}{I})^2}]^{1/2} = \frac{1}{\sqrt{2}} [\frac{\hat{\tau}}{\mu\omega_1}] \qquad (8)$$

Letting $\omega_1 = \omega_r + \varepsilon$ where $\varepsilon \ll \omega_r$, equation (8) can be solved for ε, giving,

$$\varepsilon = \frac{\mu}{2I} [- \frac{\mu}{2I\omega_r} \pm \{ (\frac{\mu}{2I\omega_r})^2 + 1 \}^{1/2}]$$

For a system with high mechanical Q, $\frac{\mu}{2I\omega_r} \ll 1$, so that to a very good approximation,

$$\varepsilon = \pm \frac{\mu}{2I} \quad (\frac{1}{\sec}) \qquad (9)$$

The band width, B.W., is twice ε, so that

$$B.W. = \frac{\mu}{I} \quad (\frac{1}{\sec}) \qquad (10)$$

The mechanical Q is given in several forms by,

$$Q \equiv \frac{\omega_r}{B.W.} \qquad (11)$$

$$Q = \frac{1}{\mu} [kI]^{1/2} \qquad (12)$$

$$= \frac{\omega_r I}{\mu} \qquad (13)$$

$$= \frac{k}{\mu \omega_r} \qquad (14)$$

The system is sustained in resonance by automatically adjusting the driving frequency so as to maintain the 90° phase angle between torque and angular response. Sensing of an off-resonance error depends upon the fact that the phase angle α between τ and $\theta(\omega)$ changes rapidly near ω_r. The rate of change of α with frequency near resonance can be obtained from equation (2) by noting that

$$\tan \alpha = \frac{\mu \omega}{I (\omega_r^2 - \omega^2)} \quad . \qquad (15)$$

The derivative of equation (15) with respect to ω, after simplification, gives the following expression for the rate of change of phase with frequency near resonance,

$$\frac{d\alpha}{d\omega} = - \frac{2I}{\mu} \qquad (\frac{radians}{radian/sec}) \quad \text{or} \quad (\frac{cycles}{Hz}) \quad . \qquad (16)$$

Other forms are

$$\frac{d\alpha}{d\omega} = - \frac{2}{B.W.} = - \frac{2Q}{\omega_r} \qquad (\frac{radians}{radian/sec}) \qquad (17)$$

$$= - \frac{1}{\pi \ B.W. \ _{(Hz)}} \qquad (\frac{cycles}{Hz}) \qquad (18)$$

$$= - \frac{114.5}{f_r} Q \qquad (\frac{degrees}{Hz}) \qquad (19)$$

$$\text{where } f_r = \frac{\omega_r}{2\pi}$$

When the system operates precisely at ω_r, then there is no change in the resonant frequency if μ changes. However, if the phase difference between torque and response is not quite 90°, there will be some error. Its magnitude may be determined as follows:

$$\frac{\partial \omega}{\partial \mu} = - \frac{\frac{\partial \alpha}{\partial \mu}}{\frac{\partial \alpha}{\partial \omega}} \qquad (20)$$

The denominator as obtained from equation (15) is:

$$\frac{\partial \alpha}{\partial \omega} = \frac{\mu}{I} [(\omega_r^2 - \omega^2) + 2\omega^2] [\frac{I^2}{I^2 (\omega_r^2 - \omega^2) + (\mu\omega)^2}] \quad . \qquad (21)$$

The numerator, also obtained from equation (15) is:

$$\frac{\partial \alpha}{\partial \mu} = \frac{\omega I (\omega_r^2 - \omega^2)}{I^2 (\omega_r^2 - \omega^2)^2 + (\mu\omega)^2} \quad . \qquad (22)$$

The quotient, after letting $\omega = \omega_r + \varepsilon, (\varepsilon \ll \omega_r)$ and after some simplification, gives,

$$\frac{\frac{\partial \omega}{\omega}}{\frac{\partial \mu}{\mu}} \simeq \frac{\varepsilon}{\omega_r} \quad .$$

But $\varepsilon = \dfrac{\partial \omega}{\partial \alpha} \Delta \alpha$ so that

$$\frac{\frac{\Delta \omega}{\omega}}{\frac{\Delta \mu}{\mu}} = \frac{\Delta \alpha}{\omega_r} \frac{1}{\frac{\partial \alpha}{\partial \omega}} \qquad (23)$$

Using equation (17),

$$\frac{\frac{\Delta\omega}{\omega}}{\frac{\Delta\mu}{\mu}} = \frac{\Delta\alpha}{2Q} \qquad (24)$$

when $\Delta\alpha$ is expressed in radians.

Equation (24) shows that the percent change in frequency compared to the

percent change in μ decreases with increasing system Q. This is one ad-

vantage of making Q as large as possible.

The peak value of torque $\hat{\tau}$ required to sustain a peak angular dis-

placement $\hat{\theta}$ at resonance is obtained from equation (7).

$$\hat{\tau} = \hat{\theta}\mu\omega_r \qquad \text{(dyne cm)} \qquad (25)$$

Or,

$$\hat{\tau} = \frac{1}{Q} (k\hat{\theta}) \qquad \text{(dyne cm)} \qquad (26)$$

It is important to note in equation (20) that $k\hat{\theta}$ is the restoring torque

provided by the torsion bars when the transducer head is twisted by an

amount $\hat{\theta}$. It is clear that another advantage of a high Q system is that

the amount of torque required to sustain an angular displacement $\hat{\theta}$ at

resonance is decreased in proportion to Q.

The torque is produced by the simple technique of current interaction

with a powerful magnetic field as is done in galvanometer movements. As

shown in Figure I, a coil of N turns is placed with its plane parallel to

the magnetic field of intensity B(webers/m^2). The coil encloses an area

S(meters)^2. When a current of I(amps) is forced through the coil, the

torque τ produced is

$$\tau = (BINS) (10^7) \qquad \text{(dyne cm)} \qquad (27)$$

When the mechanical system has a large Q, sufficient torque is provided by

this technique to drive the system.

D. Temperature Compensation

The thermoelastic coefficient (TEC) as used here is defined as the change in elastic modulus without correction for the effects of thermal expansion. This is a convenient definition because it is the form often given in technical bulletins. (Internation Nickel Company, Inc., 1963.)

The moment of inertia I of the transducer head is proportional to its height h and the fourth power of its radius R. The expression for angular frequency ω can be written as

$$\omega_r = C \sqrt{\frac{k}{hR^4}} \tag{28}$$

where C is a constant. When (28) is differentiated with respect to temperature T, the following expression results:

$$\frac{1}{\omega_r} \frac{d\omega_r}{dT} = \frac{1}{2} [\frac{1}{k} \frac{dk}{dT} - 5\alpha_T] \tag{29}$$

where $\frac{1}{\omega_r} \frac{d\omega_r}{dT}$ represents the temperature coefficient of resonant frequency, $\frac{1}{k} \frac{dk}{dT}$ is the TEC for the torsion bars and $\alpha_T \equiv \frac{1}{h} \frac{dh}{dT} = \frac{1}{R} \frac{dR}{dT}$ is the thermal expansion coefficient of the transducer head. If a torsion bar material is chosen which has a TEC which is positive and equal to five times the thermal expansion coefficient of the transducer material, then, theoretically at least, the temperature coefficient of resonant frequency will be zero. Such a material is Ni-Span-C Alloy 902, a product of the International Nickel Company. With the proper amount of cold work and heat treatment, this alloy can be given a wide range of TEC's as shown in Figure II. This technique of balancing a TEC against a thermal expansion coefficient in order to reduce the effects of temperature changes has been used successfully by watchmakers and manufacturers of mechanical frequency standards such as

tuning forks. More will be said in the <u>Performance</u> section about the success of the technique in the <u>in situ</u> densitometer prototype.

DESCRIPTION

A. Transducer Assembly

Figure III shows the working parts of the densitometer in assembled form. The transducer head is machined from a solid block of #304 stainless steel for dimensional stability and for resistance to attack by seawater. The surface is not coated or passivated in the prototype, but this could be done to eliminate frequency drift if long exposure to corrosive environments is expected. Although stainless steel has a moderate thermal expansion coefficient, its effect on frequency can be eliminated by properly choosing the TEC for the torsion bars, as is demonstrated in equation (29). The moment of inertia of the transducer head itself is 2.64 times the moment of inertia of the virtual water mass so that the percent change in frequency is attenuated by a factor of 7.3 over the percent change in fluid density, as is shown in Table I. The thickness of the vanes and web are designed so that flexure of the head itself at any point contributes less than 1% to the total displacement due to twisting of the torsion bars.

Figure IV is a photograph of the assembled densitometer unit. The torsion bars are rigidly attached to the two end plates so that the torsion coil is positioned between the shaped pole pieces in the magnetic field. The framework is rigid so that there is negligible twisting in it when torque is applied to the transducer head. The entire unit is open to allow fluid to flush freely through the transducer. This feature insures a rapid response to density changes in the surrounding fluid.

B. Torsion Coil

The 400 turns of magnet wire carrying a peak current of 70 ma. at the resonant frequency in a magnetic field of about 3,000 Gauss supply sufficient

torque to twist the transducer through an angle of 0.5×10^{-3} radians (Table I). At this small amplitude the surface acceleration at any point of the vanes is so small that no cavitation occurs. The energy dissipated in the coil is .22 watts or .053 cal/sec. A slight flushing rate is sufficient to remove this heat from the vicinity of the transducer, eliminating possible error due to local heating. The coil is encapsulated in epoxy to protect it from the water during immersion.

C. Strain Gage Bridge

Angular displacement of the transducer head is sensed by a 4-arm active semiconductor strain gage bridge as shown in Figure V. Specifications for the gages are given in Table II. The gages are mounted on opposite faces of two flats at the base of one of the torsion bars. Their orientation at 45° with respect to the torsion bar axis and their electrical connection give maximum sensitivity to torsional stresses and greatly attenuate signals due to flexure of the bar. This insures that possible flexural modes of oscillation will not be excited. The location of the strain gage flats on the torsion bar is shown in Figure VII.

D. Feedback System

Resonance is sustained by feedback as shown in Figure VIII. The sequence of events by which the resonant frequency is achieved occurs as follows. The voltage-controlled oscillator (VCO) begins at a frequency that is near to but not exactly at the resonant frequency. It provides a signal to the current source which in turn sends a current through the torsion coil. The torque produced by this current forces angular displacements of the transducer head. The strain gage bridge emits a signal proportional to and in phase with the displacements.

After the bridge signal is amplified by the strain gage amplifier, all D.C. is removed, and it is turned into a square wave. This signal is applied to one input of the phase comparator. The VCO signal, after having been shifted in phase 90° by a single integration, is applied to the other input of the phase comparator. Once each cycle the phase comparator generates a pulse of constant amplitude whose width is proportional to the difference in phase between the two inputs. If the phase is leading, the pulse appears on the upper line, and vice versa. The up-down integrator accepts these pulses and adjusts its output level accordingly so as to bring the VCO to the exact resonant frequency.

This type of proportional control in the feedback loop produces a very tightly locked resonant system. Because a correction is applied once each cycle, any instantaneous error is reduced by averaging over a number of cycles. Having a local oscillator whose frequency need be adjusted only slightly has the added benefit of allowing the system to adjust rapidly to sudden changes in fluid density.

The electronic package containing the feedback system is shown in Figure IX. The first six cards comprise the feedback electronics. The last four cards are for voltage supplies and cable-driver units which were omitted for the bench testing. It is visualized that as an ocean-going instrument, this device will be able to operate on a single conductor cable, D.C. power and A.C. signals flowing in opposite directions through a common wire. The return can be via a seawater path. The diameter of the package is such that it will fit easily inside a standard six inch I.D. pressure case.

Figures XIII through XVIII are schematic diagrams for the feedback system electronics.

E.   Response Time

Actual response time is difficult to determine. Direct measurements are not feasible because step changes in density are not simple to achieve. It is not easy to calculate response time either because of the type of feedback system used. Some idea of the speed with which the mechanical system responds to changes in the environment can be obtained, however, by observing the time required to regain resonance after the transducer head is held rigidly for a moment so that its motion is nearly stopped. This kind of test has revealed that the system is able to regain its resonant condition typically within about one second after the transducer head is released.

F. Operation

Because of time limitations, it was not possible to completely waterproof the strain gages and the torsion coil leads on this prototype. This is a simple matter for the next model, however. The consequence has been that this unit can be immersed only up to and including the magnet pole pieces. The U-shaped portion of the magnet which surrounds the strain gages should remain above the water level. Before complete testing proceeded, careful checks were made to make certain that changes in water level, once the transducer head itself was submerged, had no noticeable effect on the resonant frequency.

PERFORMANCE

A. Testing Procedure

Measurements of temperature coefficient of resonant frequency were performed six times. The first test was with the densitometer operating in air. It was placed in an insulating plastic foam box along with a heater and a small fan to keep the air thoroughly mixed. The temperature was monitored continuously by means of a thermistor and a strip chart recorder. A mercury thermometer was installed through the wall of the box so that the thermistor reading could be checked periodically. Temperature could be read easily to $\pm$ .05° C. Over a period of three hours the temperature was gradually raised from 22° C to 25° C. This slow rate of change of temperature allowed the densitometer to maintain thermal equilibrium. A Beckman Model 6126 preset counter was used to determine the average period of the resonant frequency. This value was printed out every 100 seconds. The Beckman counter was used in all tests.

The second test was with the unit in water in a plexiglass tank. An immersion heater was used to raise the temperature from 23° C to 27° C over a period of two hours. A propeller kept the water well-mixed. Temperature was recorded continuously by means of a thermistor and strip chart recorder. A mercury thermometer was used as a check. Average period was determined by the Beckman preset counter.

The other four temperature coefficient tests were made while the unit was undergoing a long-term stability test which lasted four days. Ice was placed in thermal contact with the water to lower the temperature to about 20° C; and over a period of six to seven hours, the temperature gradually returned to room temperature (23° C). The water was mixed continuously to eliminate temperature gradients, and data were logged as before.

The long-term drift test was run in the same plexiglass tank for four days in pure water. The transducer head was carefully cleaned to remove from the surface any traces of material that might cause its moment of inertia to change. Temperature was recorded continuously and period was printed out every 100 seconds. As before, a propeller kept the water completely mixed.

A test was made to determine if water motions caused any frequency shift or if they generated noise that would show up as erratic readings of average period. With the densitometer immersed in water in a small bucket, a propeller driven by a small motor was used to churn the water as hard as possible without mixing in air. The state of motion resembled that of a rolling boil. This was a very important test for a device intended for use in situ since it must be able to perform its function regardless of its motion relative to the fluid.

It was not possible to perform pressure sensitivity tests on this prototype because of the possibility of destroying the unprotected strain gages by complete submersion. It is felt, however, that the pressure coefficient will be small because the unit is constructed of solid steel material whose characteristics are not expected to change significantly under pressures encountered in the ocean. Because there are no voids within the transducer, a pressure increase cannot cause deformation, a primary source of pressure sensitivity in other types of instruments.

The sensitivity of the densitometer to density changes in the fluid was determined by operating the unit in 10,000 $\pm$ 10 grams of distilled water to which was added in small increments accurately weighed amounts of NaCl. The salt was weighed to $\pm$ 0.1 mg. in thirty separate sealed containers. The total weight of salt used was about 700 grams. Sum total of weighing

errors for the thirty containers was less than 3 mg, so that relative

salinity error was less than 3×10^{-7}. Absolute salinity had an un-

certainty of $\pm 1 \times 10^{-3}$ because the exact weight of water was known only

to ± 10 gms. Period of resonance was recorded as the salinity was in-

creased in 25 steps (more than one container was used in some additions)

until all 700 grams of salt had been used. As before temperature was

monitored and the water stirred vigorously. Density was calculated from

the amount of salt added by interpolating the data published in the In-

ternational Critical Tables for NaCl solutions at various temperatures.

Relative densities computed by this technique are accurate to about

$\pm 2 \times 10^{-5}$ gm/cm^3. The absolute density is in error by an amount equal

to the initial uncertainty in quantity of water. The increase in density

achieved was about 5%.

B. Results

The six tests for the temperature coefficient of resonant frequency

gave values of $\frac{\Delta\omega_r}{\omega_r \Delta T}$ between $121 \times 10^{-6}/^\circ$ C and $147 \times 10^{-6}/^\circ$ C. Although

this is higher than anticipated in the design, it does not detract from

the potential usefulness of this device if temperature is measured to 0.1° C

and the resonant frequency corrected. There is also the promise of re-

ducing the temperature coefficient significantly in the next version of

the instrument by the technique discussed in the theory.

The drift test showed that there was no temporal drift of frequency

distinguishable above the effects of temperature changes. This implies

that the characteristics of the materials used in the construction of

this device are stable (at least over four days of continuous operation)

and that they do not tend to age or creep. At one point in the test,

drift became apparent, but this was traced to what appeared to be a small

amount of biological growth on parts of the transducer head. Once this growth was removed with a soft brush, the resonant frequency returned to normal and the drift disappeared.

The test to determine the effect of water motions showed no apparent change in resonant frequency and no increases in noise due to churning of the water.

A plot of the data showing period normalized to read approximately in parts per million plotted against water density is shown in Figure X. Normalization was accomplished by multiplying true period by 478. When period is plotted directly against ρ on a log-log scale, a slight curvature is evident. The reason is clear from equation (6). For small values of ρ, log P_r asymptotically approaches the constant $\frac{1}{2}$ log K_1, while for large values of ρ, log P_r asymptotically approaches the line given by $\frac{1}{2}$ [log K_2 + log ρ]. For intermediate values of ρ, the line curves to meet the asymptotes. Data are not plotted below ρ = .004 gm/cm^3. It was not possible to extrapolate below this value because the NaCl tables used did not give density for concentrations of less than 1% salt.

A more revealing plot is of period versus K_1 + K_2 ρ as in equation (6). Two data points were chosen from Figure X near the end points of the plot. These values were used in equation (6) to compute K_1 and K_2. The results are

$$K_1 = 0.73809$$
$$K_2 = 0.26476 \ .$$

Using these two values, K_1 + K_2 ρ was calculated for all the intermediate points. Figure XI is a plot of the results. It is a straight line with a slope of one-half, as predicted in the theory. This means that over the range of densities tested, the resonant frequency follows the theoretical

square root law. From the slope of the line the relative sensitivity is computed to be $\frac{\Delta\omega}{\omega} = \frac{1}{7.5} \frac{\Delta\rho}{\rho}$. This result agrees well with the value of $\frac{1}{7.3} \frac{\Delta\rho}{\rho}$ computed by a separate technique in Table I.

Figure XII is a plot of period versus time. Period was normalized as before by multiplying true period by 478. Time zero is the instant at which an addition of salt was made near the propeller which was used for mixing. Enough salt was added to raise the average density of the water 750×10^{-6} gms/cm^3. The initial 10-second delay is the time required for the first parcels of salty water to reach the transducer head. As mixing continued, the water density at the head continued to increase causing the period of resonant frequency to follow. Period was printed out once each second and has been plotted at five-second intervals for convenience. The rate of change of density was greatest between 20 seconds and 40 seconds after the addition. After 70 seconds the water was almost completely mixed. Figure XII is not related to the response time of the density transducer which is estimated to be about one second. It actually shows the mixing time for the ten liters of water in the tank. Its significance, however, is that it demonstrated the kind of direct sensitivity to density changes that can be achieved with a sensor of this design.

The temperature coefficient of resonant frequency is about 140×10^{-6}/° C, a value about 3 times higher than called for in the initial design. It is not so high as to affect the usefulness of this device as a density transducer, however. But because the temperature coefficient is now the primary factor limiting greater measurement precision, its reduction deserves further consideration. There are several factors that could cause the temperature coefficient to be larger than expected. The first is that

the TEC for the Ni-Span-C torsion bars may not be as specified, perhaps because of excessive heating or mechanical overwork during the machining process. Another is that a slight torsional reaction in the supporting framework might be causing the unit to show a temperature coefficient related to the TEC of the framework as well as to the TEC of the torsion bars. Slight longitudinal forces on the torsion bars due to differential expansion may have some effect also. It is felt, however, that the most likely cause is a slight misalignment of the supporting framework. The resulting slight flexure of the torsion bars would effectively change the torsional spring constant by an amount depending upon its magnitude. Any dimensional change in the framework with temperature would cause the torsion bars to take a slightly different bend. The result would be a temperature dependence in resonant frequency.

CONCLUSIONS

The prototype model _in situ_ densitometer described here shows
strong potential. It is directly sensitive to fluid density, a funda-
mental physical property. It provides a continuous signal whose instan-
taneous frequency is proportional to the _in situ_ density of the fluid.
Taking into account the present temperature coefficient, the largest
source of error, the device can read density with a precision of
$\pm$ 2 x 10^{-4} gm/cm^3 if temperature is read to 0.5° C. In its present
form it is useful as an oceanographic tool, and with the improvements
suggested, it may be able to meet or even surpass the $\pm$ 1 x 10^{-5} gm/cm^3
precision (Cox, 1965) of present techniques.

Because of its basic design, this instrument is not limited to
oceanographic applications. It may be used for density measurements in
a wide variety of fluids.

STRAIN GAGE FLATS

TORSION BAR

TORSION COIL

MAGNETIC FIELD

TRANSDUCER HEAD

TORSION BAR

BASE PLATE
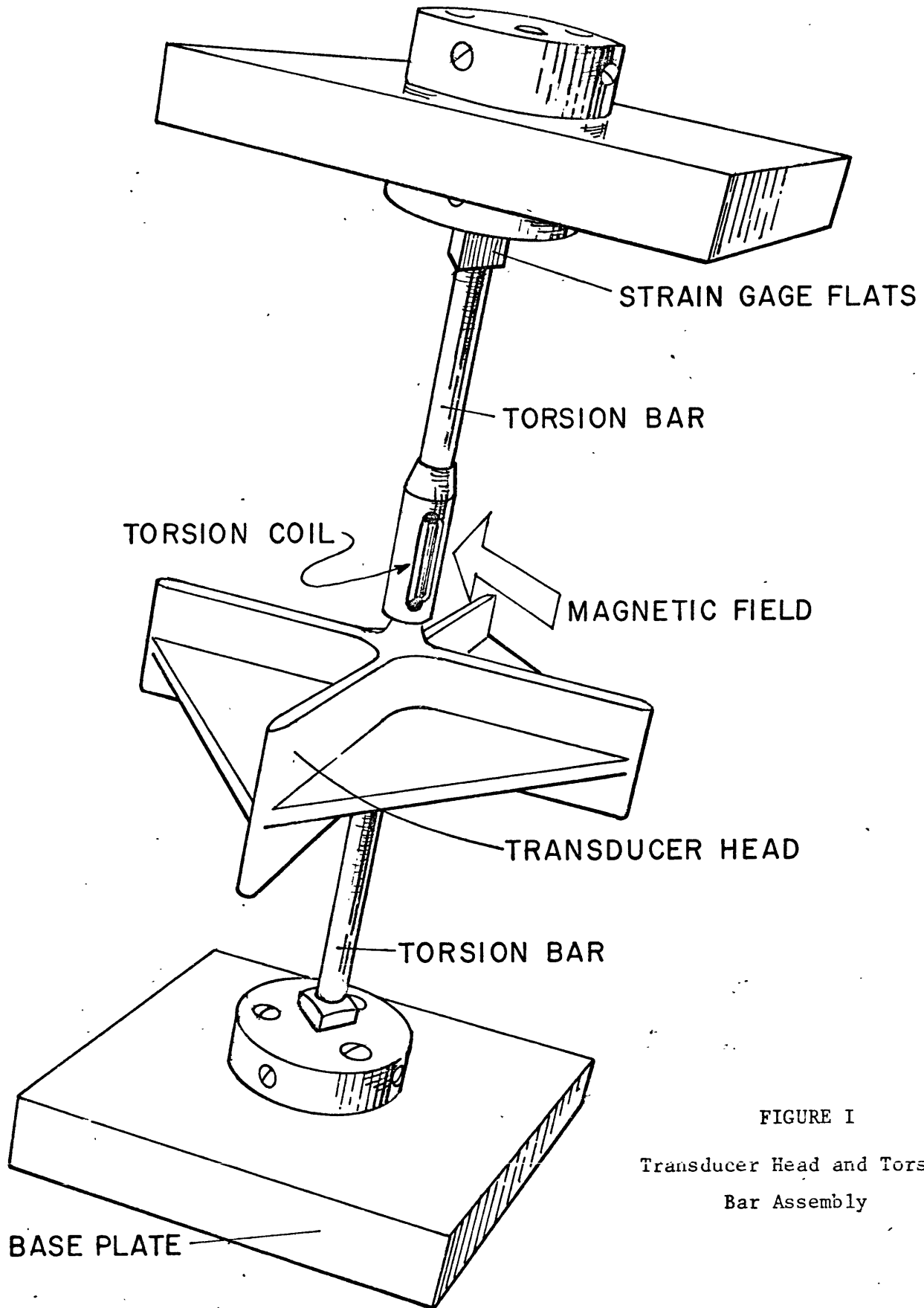
FIGURE I

Transducer Head and Torsion
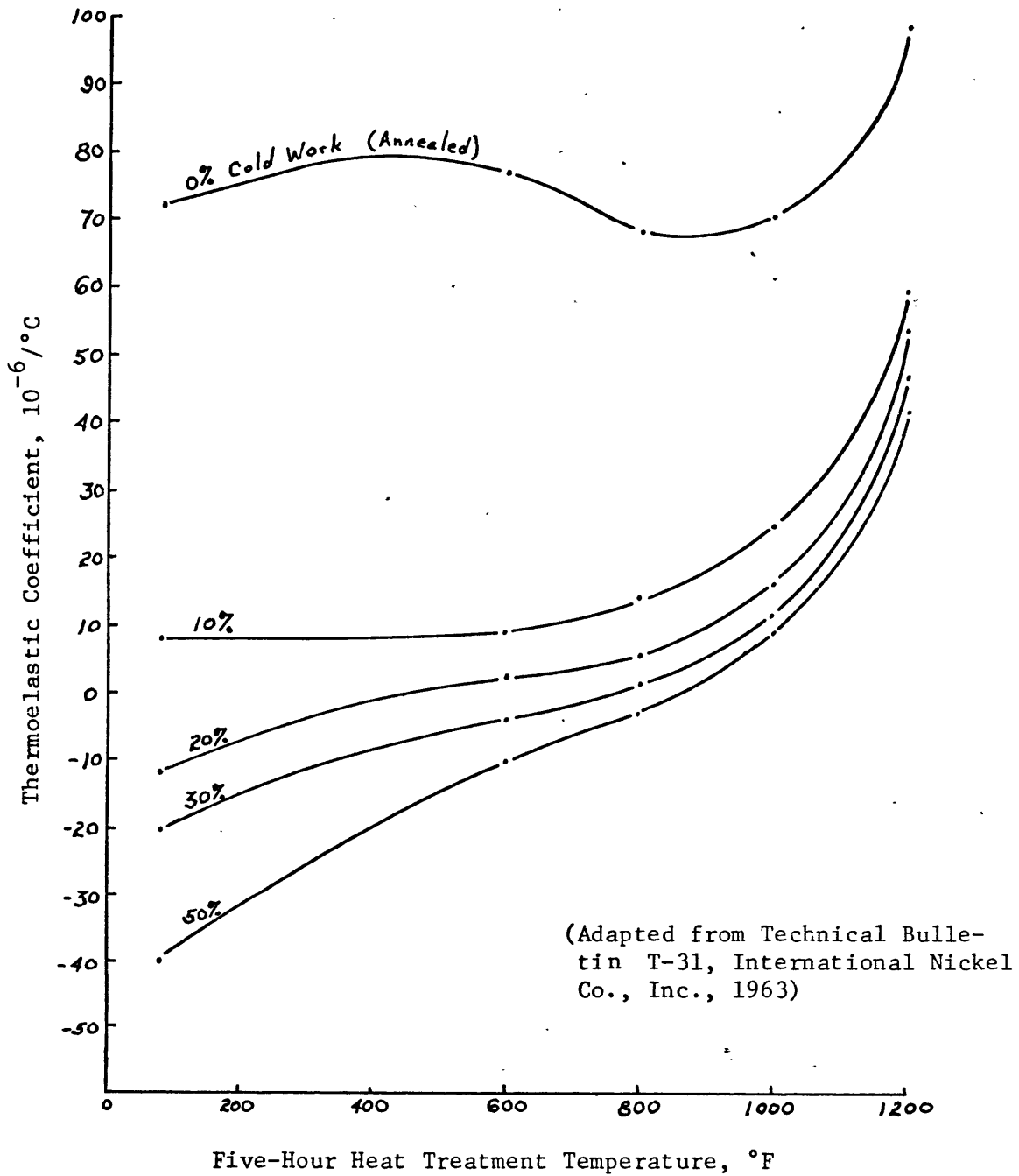
Bar Assembly
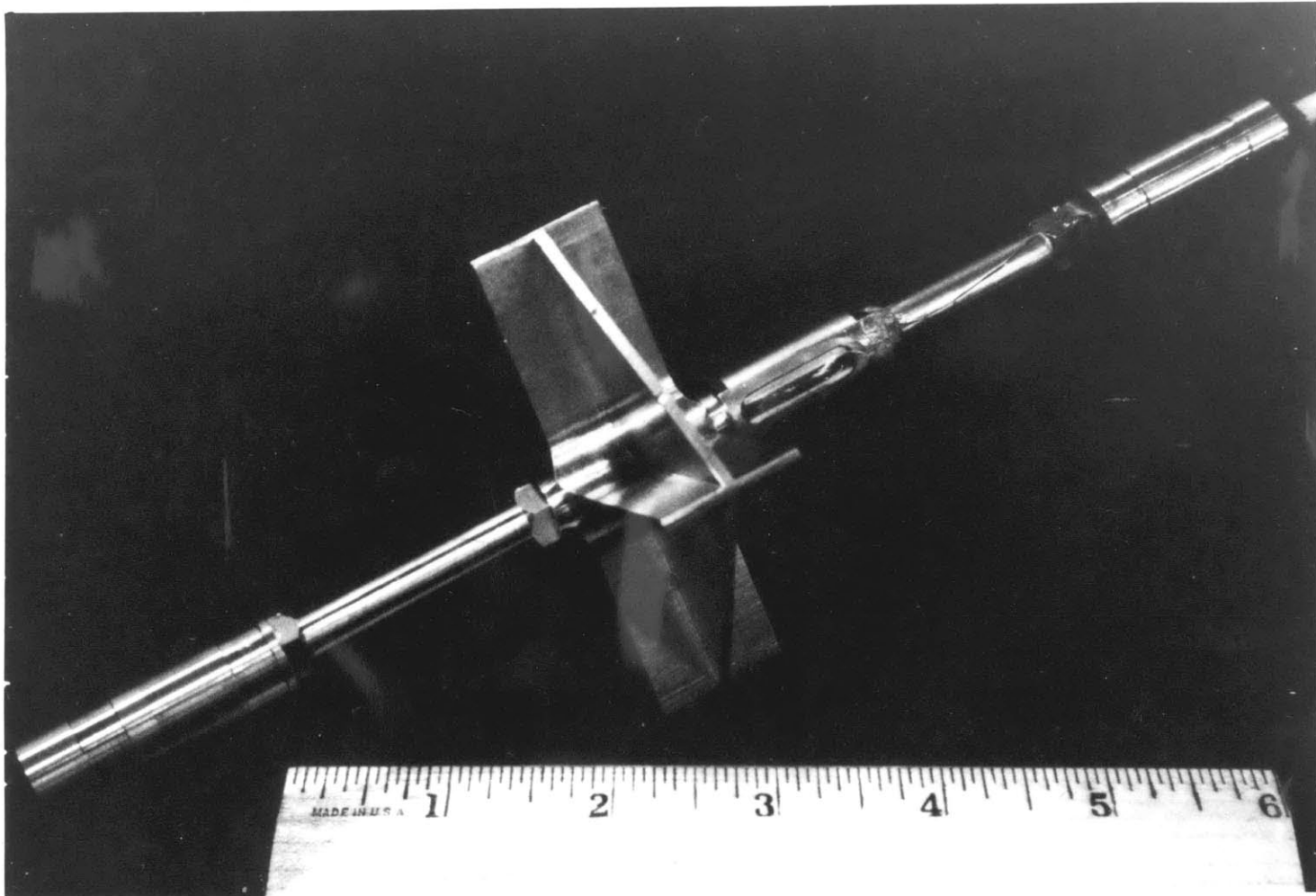
FIGURE II

Thermoelastic Coefficient of Ni-Span-C Alloy

FIGURE III

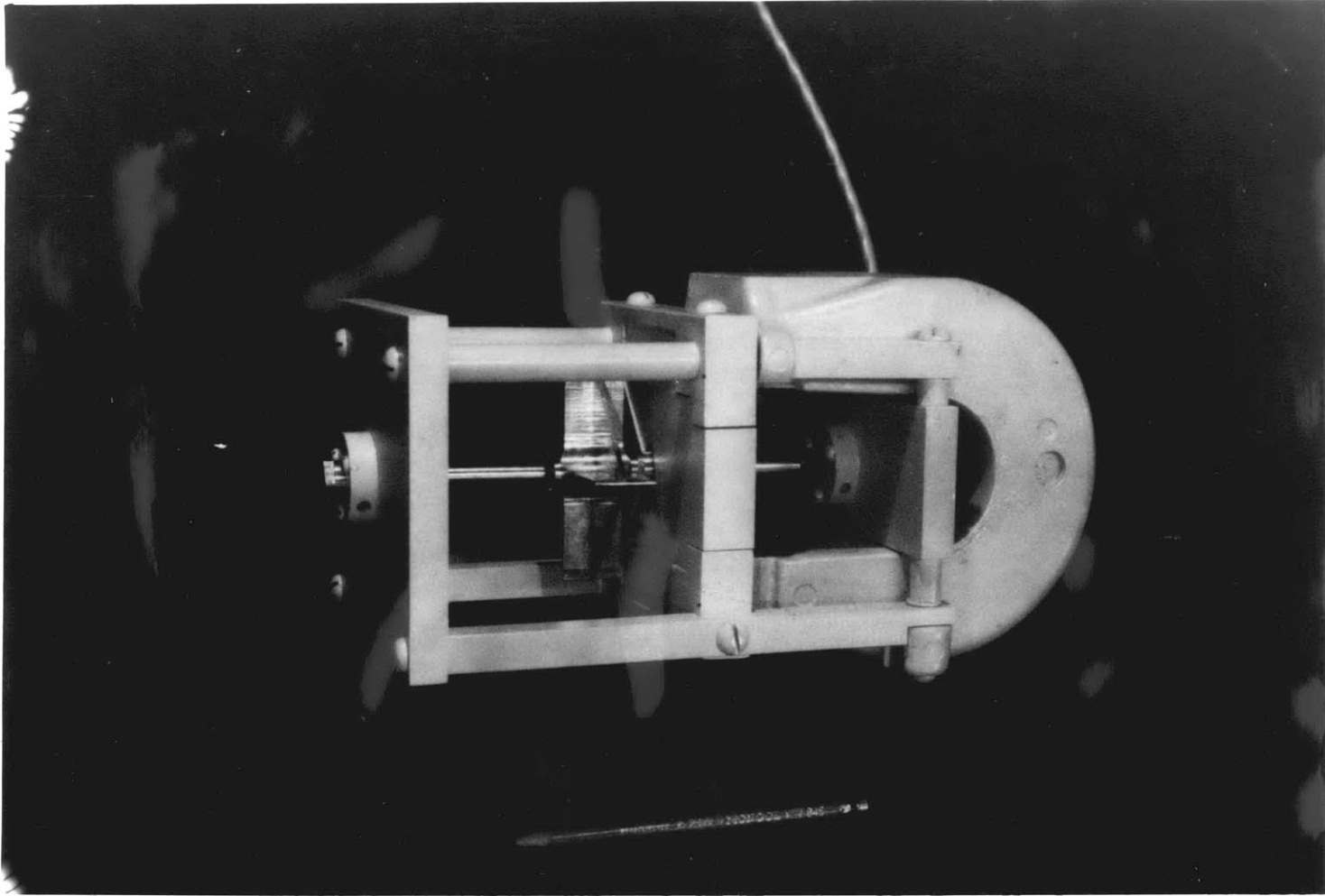Transducer Head and Torsion Bar Assembly
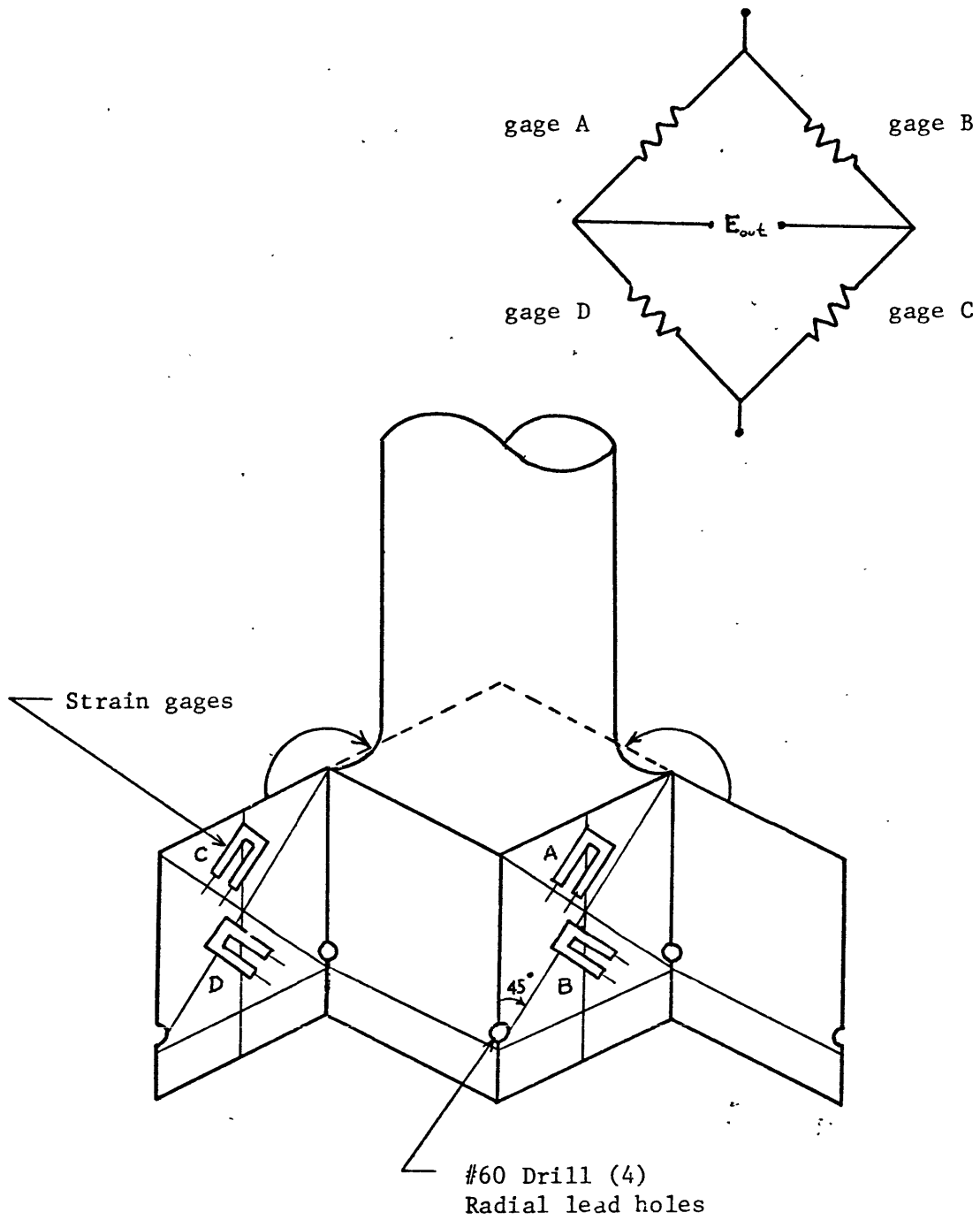
FIGURE IV

Assembled Densitometer Transducer

Strain Gage Bridge

gage A

gage B

E_{out}

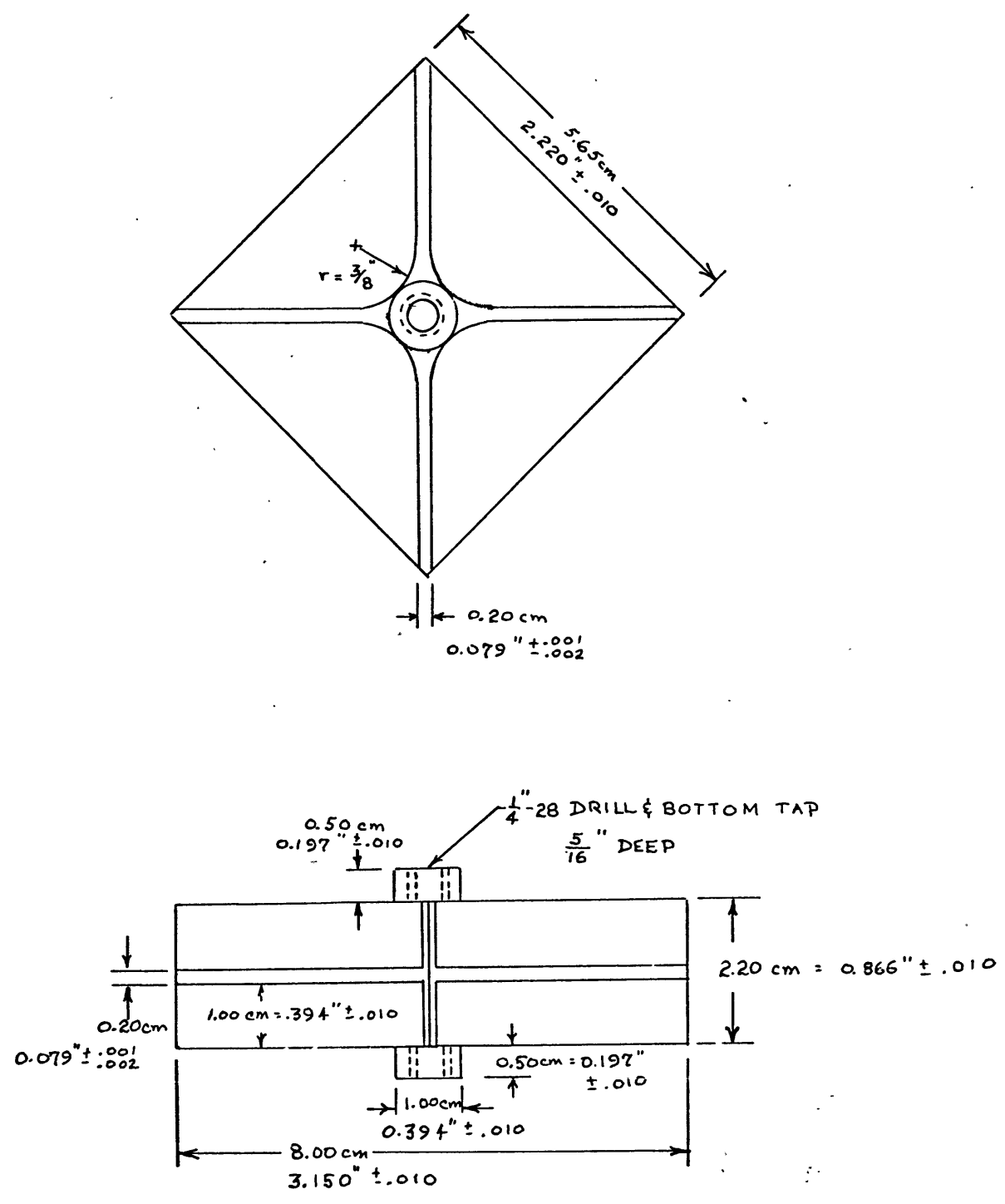gage D

gage C

Strain gages

C

A

D

45°

B

#60 Drill (4)
Radial lead holes

FIGURE V

Strain Gage Bridge

5.65 cm
2.220" ± .010

r = 3/8"

0.20 cm
0.079" ± .001
    ± .002

1/4"-28 DRILL & BOTTOM TAP
5/16" DEEP

0.50 cm
0.197" ± .010

2.20 cm = 0.866" ± .010

1.00 cm = .394" ± .010

0.20cm
0.079" ± .001
      ± .002

0.50cm = 0.197"
       ± .010

1.00cm
0.394" ± .010

8.00 cm
3.150" ± .010

FIGURE VI

Transducer Head

FIGURE VII

Torsion Bar

Input
From
Strain
Gage
Bridge

```
Strain Gage          D.C. Rejection &
Amplifier            Squaring Amp.
```

```
Voltage-             Phase             Up-Down
Controlled           Comparator        Integrator
Oscillator
```

Control Voltage

```
Current
Source
```
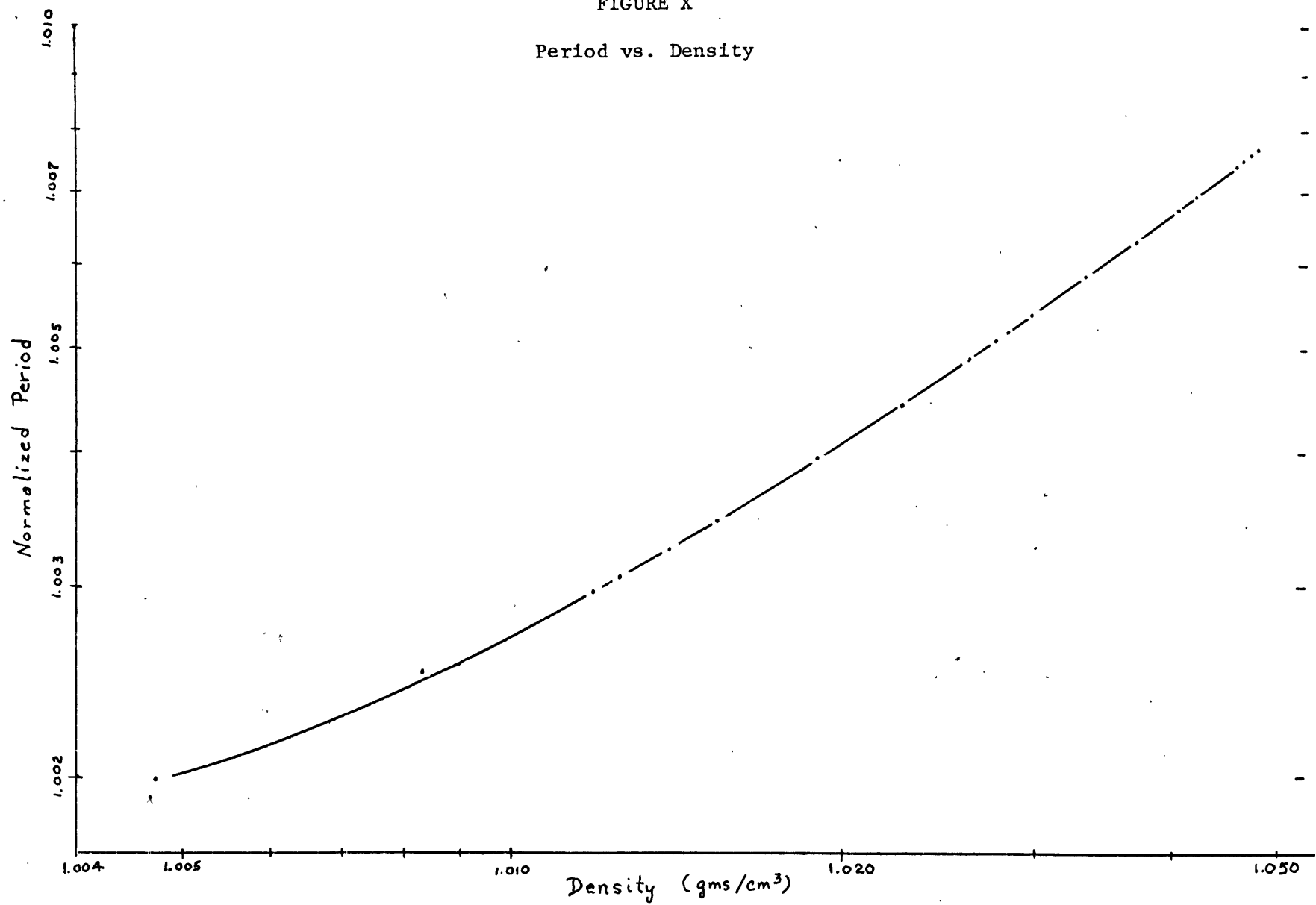
Output to
Torsion Coil
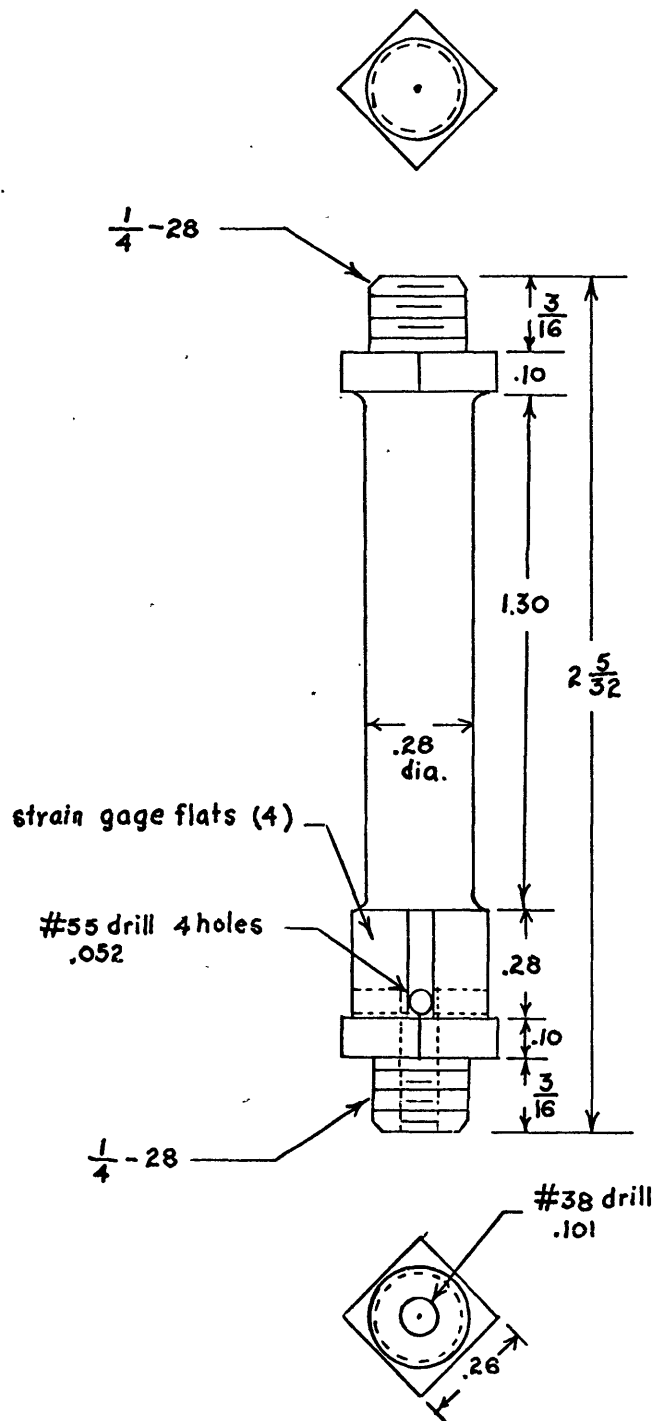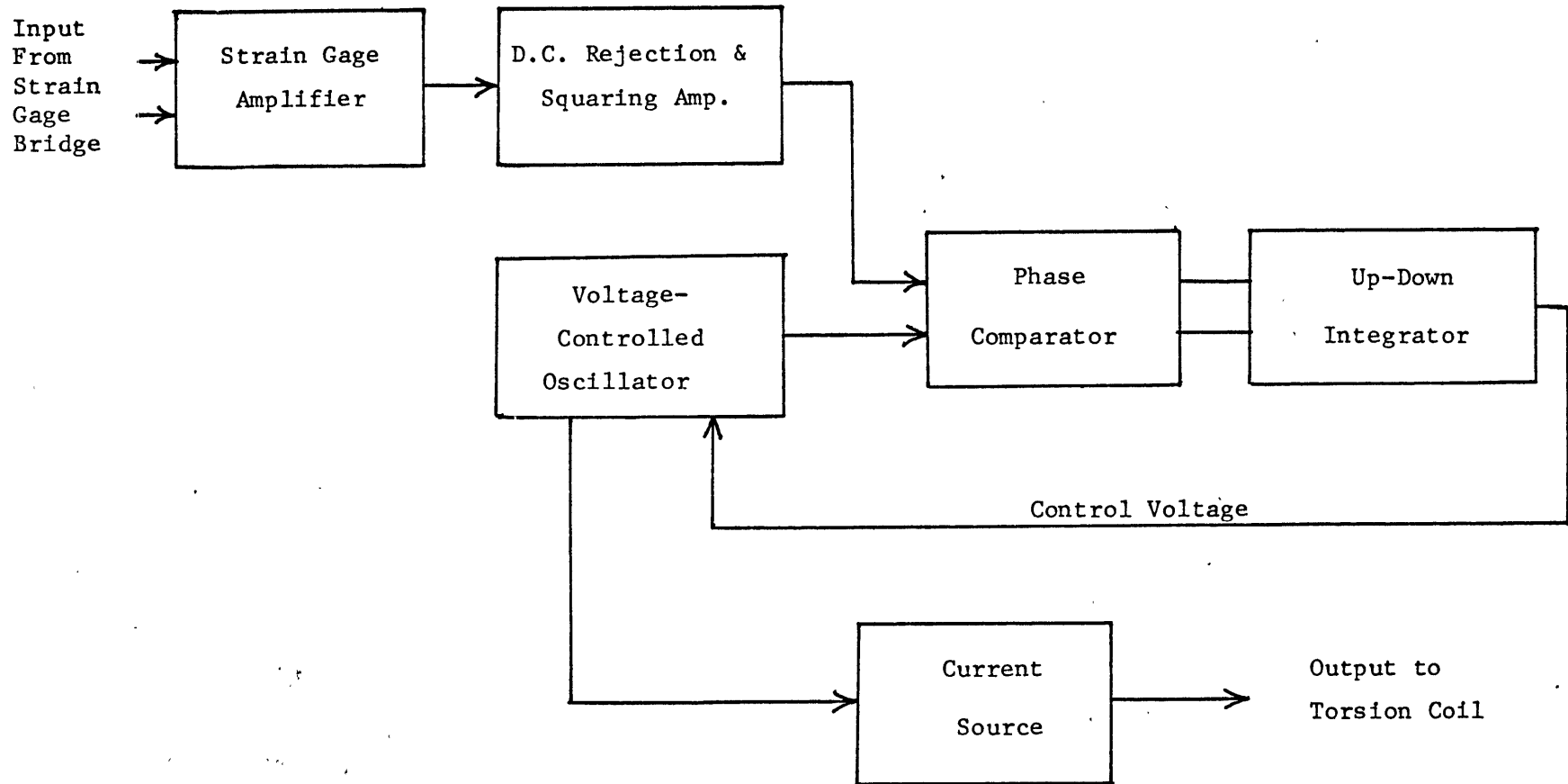
FIGURE VIII

Feedback System
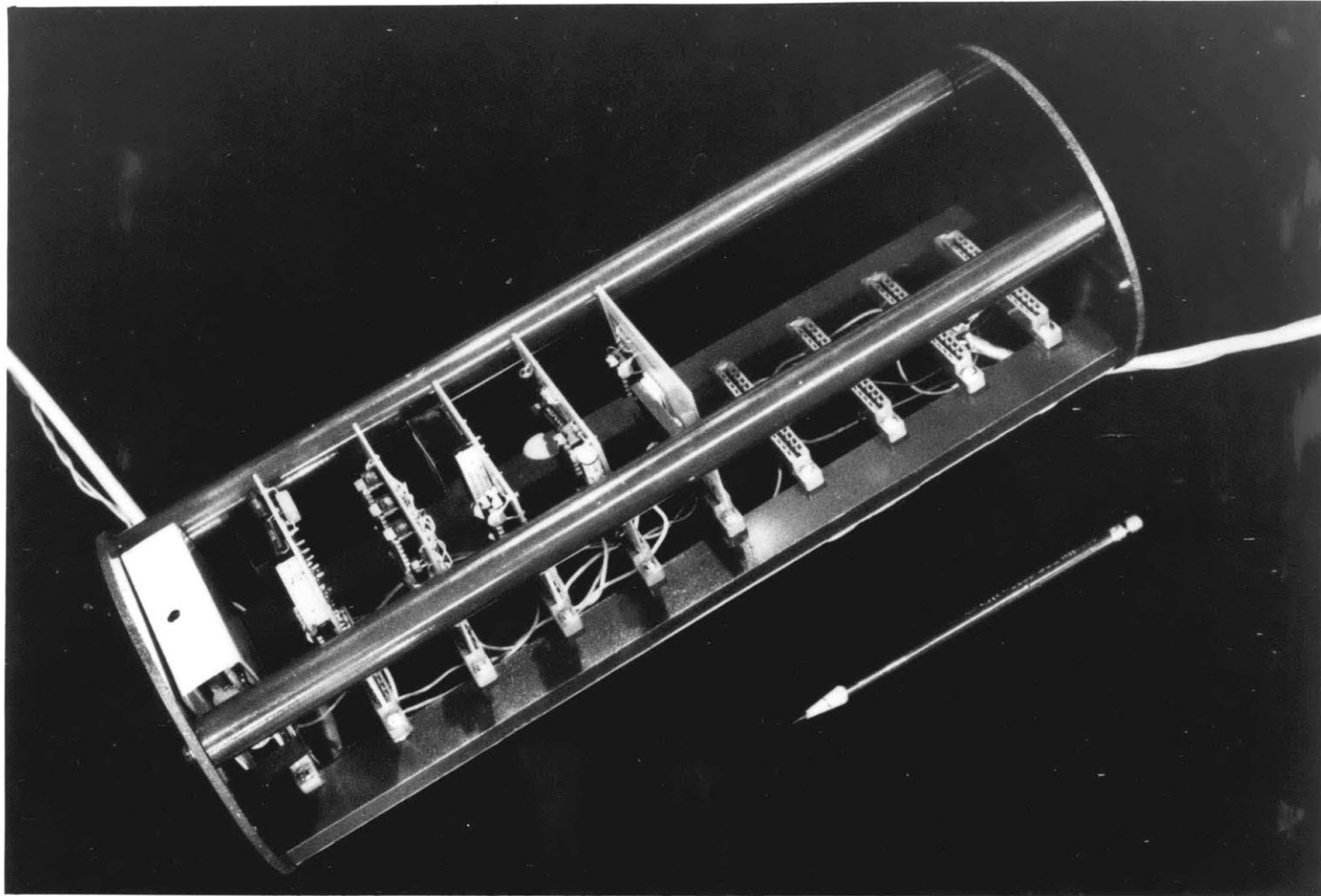
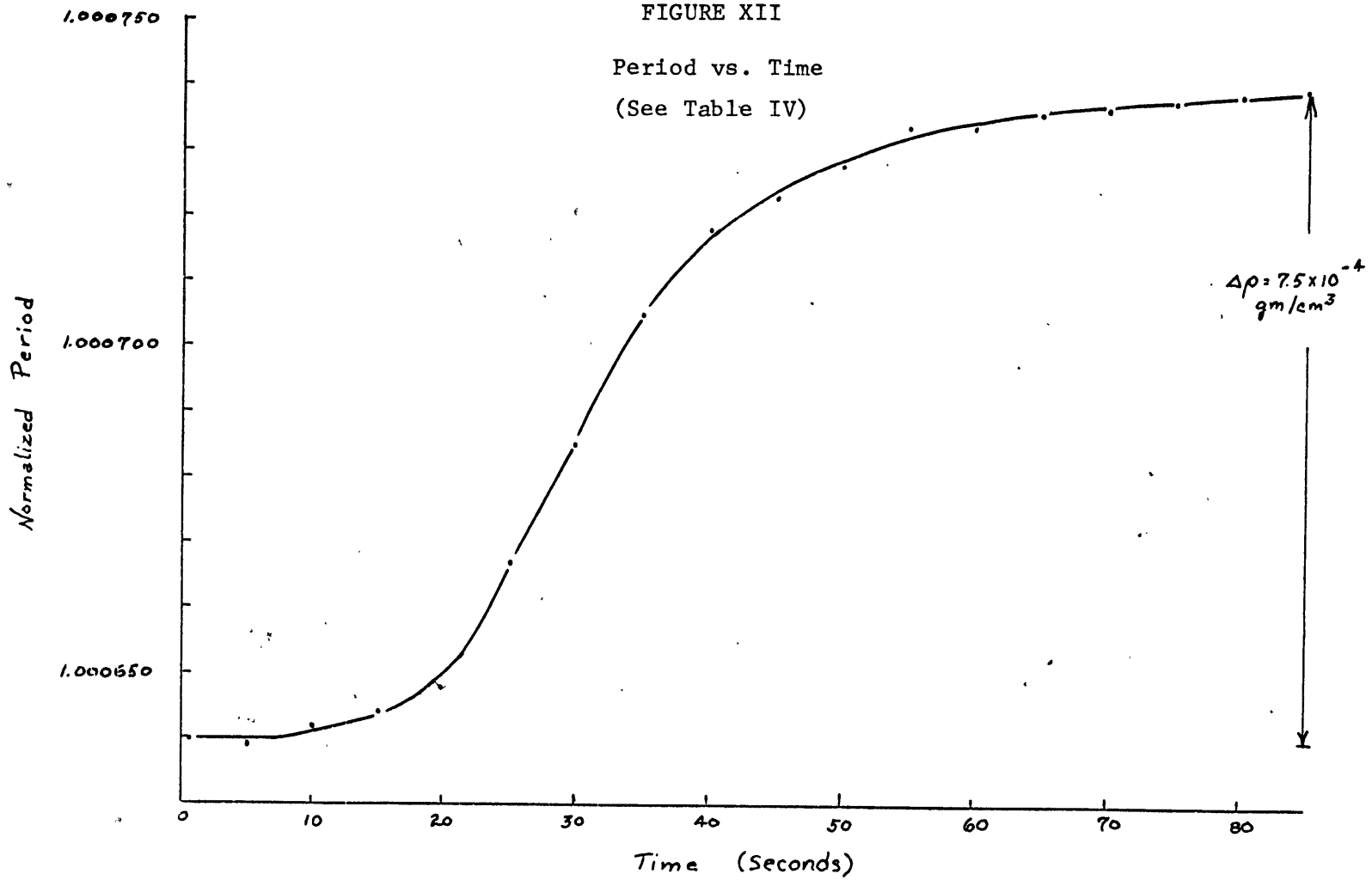FIGURE IX

Electronic Package

FIGURE X

Period vs. Density
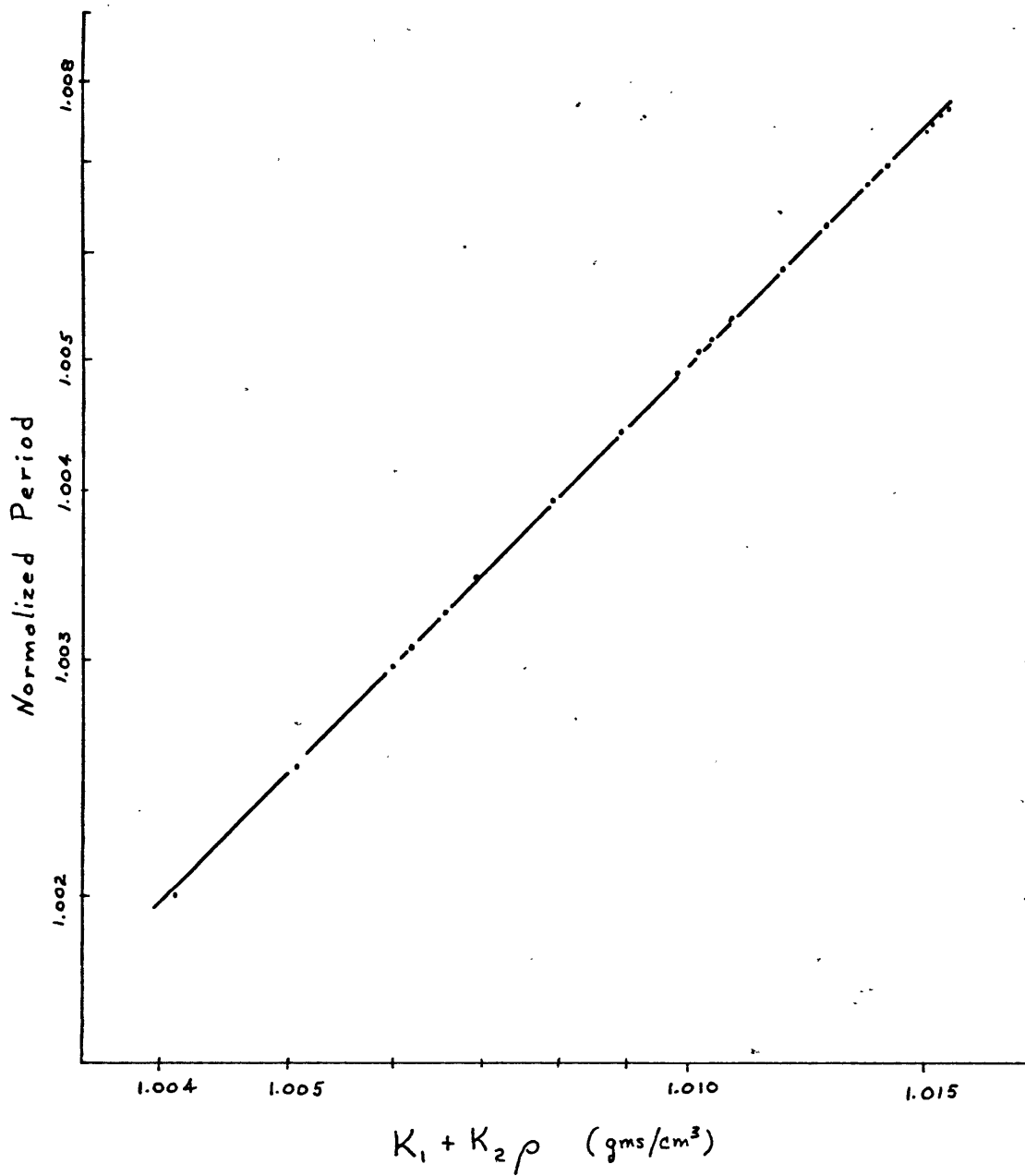
FIGURE XI

Period vs. $K_1 + K_2\rho$

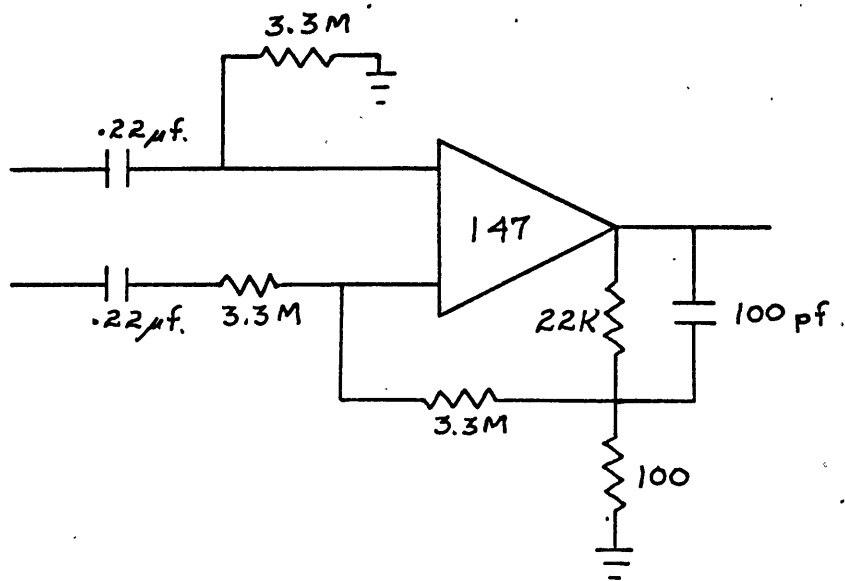(See Table III)

FIGURE XII

Period vs. Time

(See Table IV)

$\Delta \rho = 7.5 \times 10^{-4}$ gm/cm^3

Normalized Period

Time (Seconds)

FIGURE XIII

Strain Gage Amplifier
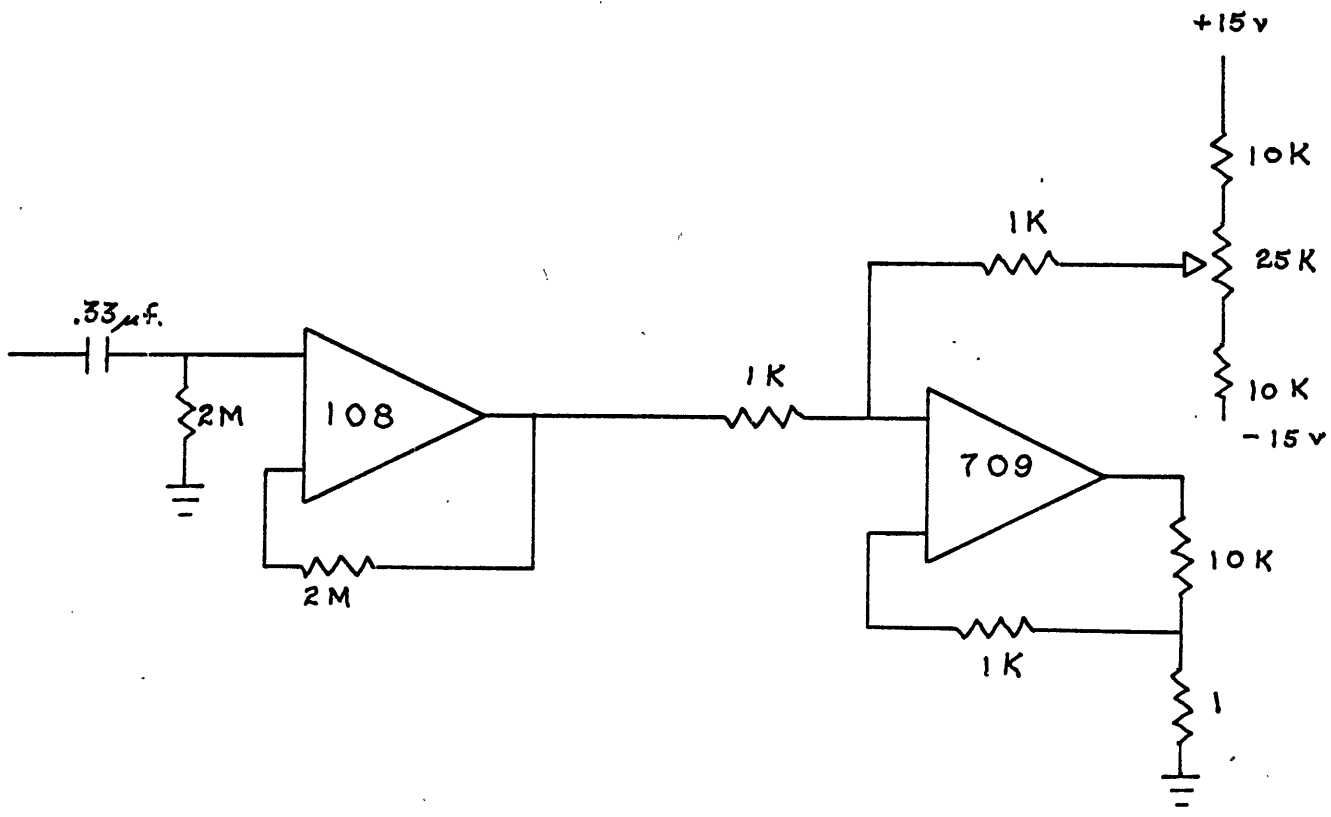
FIGURE XIV

D.C. Rejection and Squaring Amplifiers

FIGURE XV
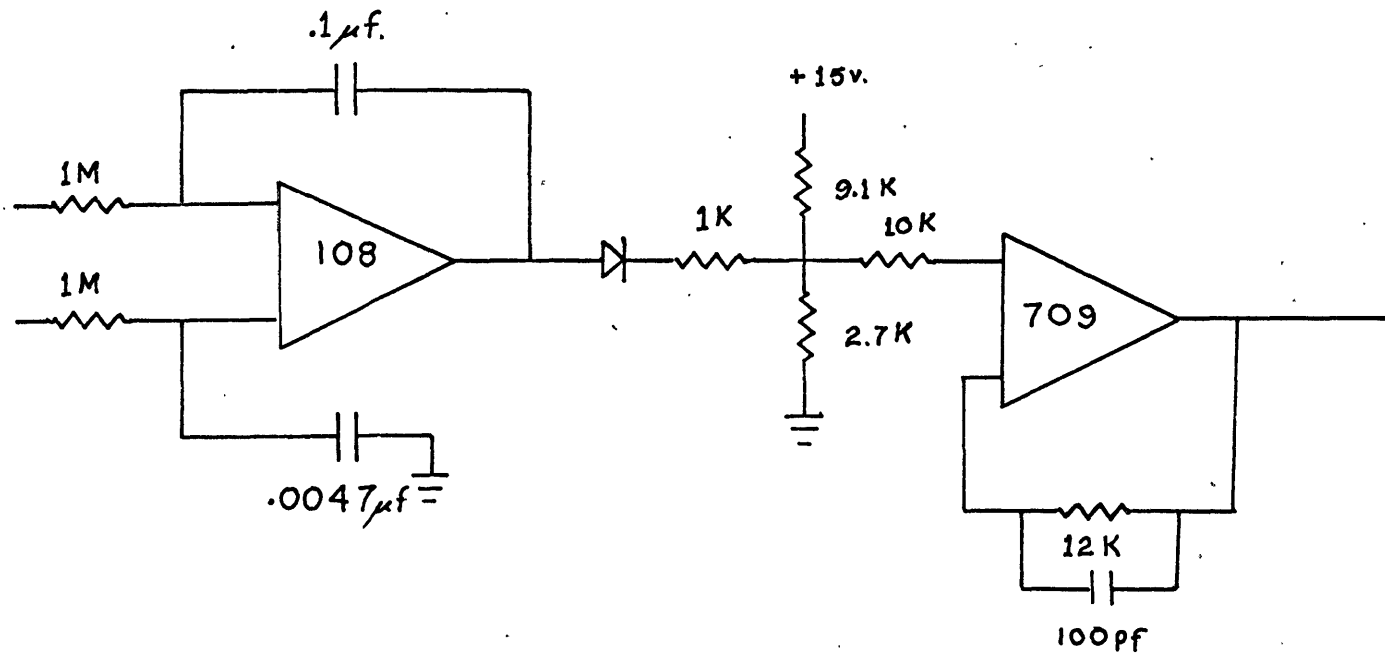
Phase Comparator

FIGURE XVI
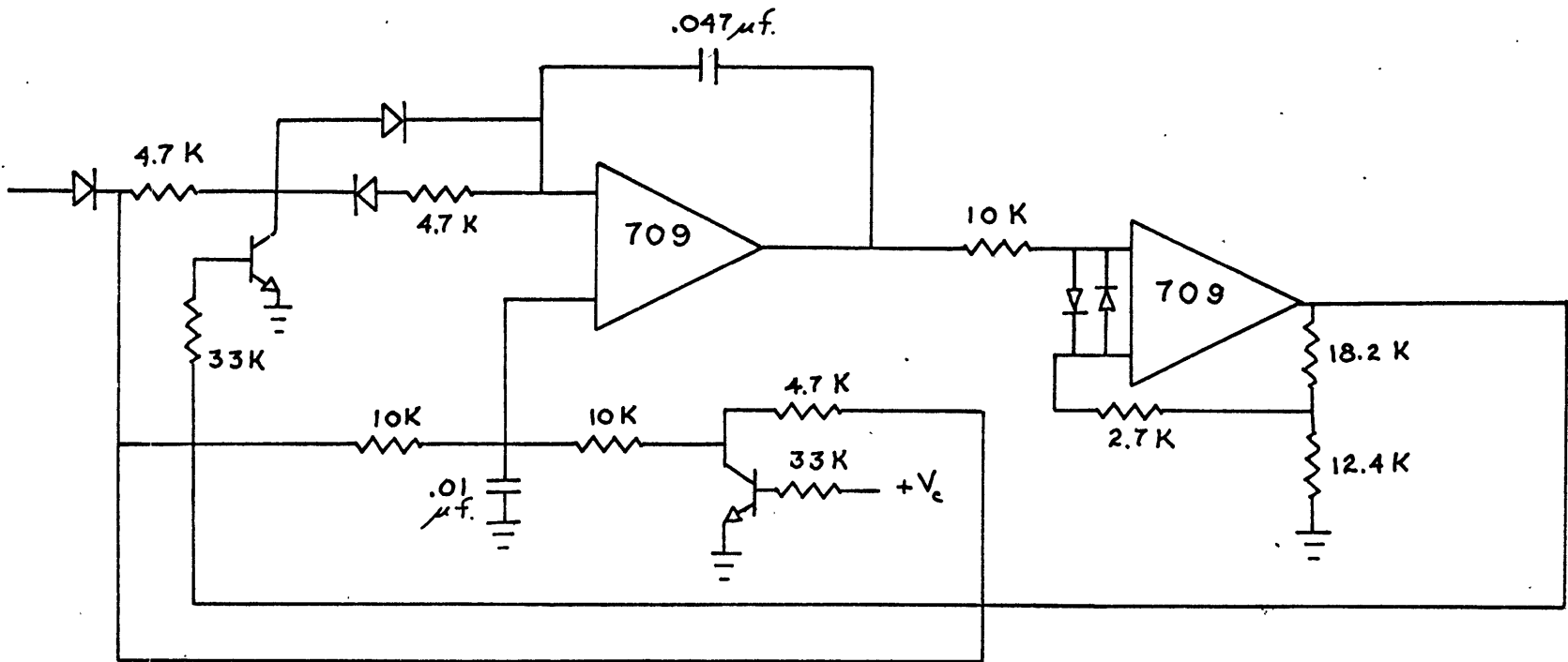
Up-Down Integrator

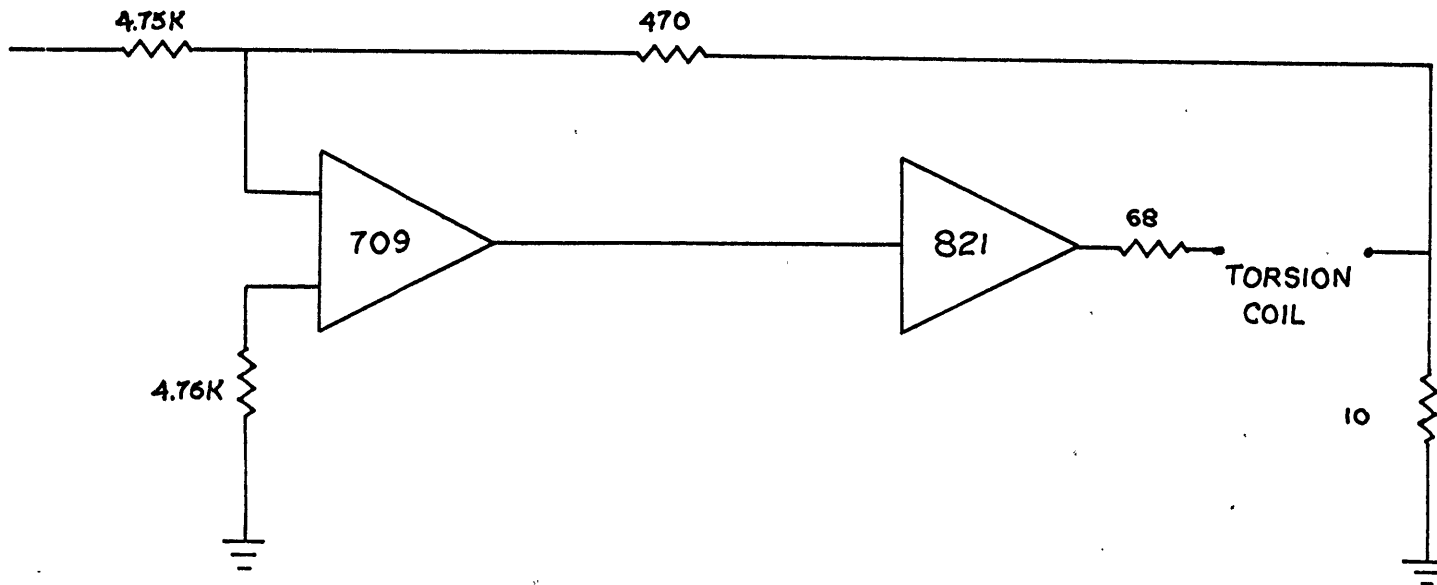FIGURE XVII

Voltage-Controlled Oscillator

FIGURE XVIII

Current Source

TABLE I

List of Computed Values

I. Data

1. Resonant frequency in air: 560 Hz

2. Resonant frequency in water: 477 Hz

3. Modulus of rigidity G of
   Ni-Span-C: 7.04×10^{11} dynes/cm^2

4. Thermal expansion coefficient
   α_T of stainless steel: 16×10^{-6}/°C

5. System Q: 239

6. System Band Width (B.W.): 2 Hz

7. Thermoelastic Coefficient of
   Ni-Span-C:
   -30×10^{-6}/°C
   to
   $+36 \times 10^{-6}$/°C
   (exact value unknown)

8. Coil Area S: $\simeq 2$ cm^2

9. Magnetic Flux Density B: 3,000 Gauss = .3 webers/m^2

10. Current: $I = 70$ ma. peak

11. Turns: $N = 400$ turns

12. Coil Resistance: $R = 87 \ \Omega$

II. Torsional Spring Constant for Torsion Bars
    (sum total for both bars)

$k = 2 \ [\dfrac{\pi a^4 G}{2\ell}]$ dyne cm $a = .355$ cm, radius

$k = 7.8 \times 10^9$ dyne cm $\ell = 4.53$ cm, length

III. Loss Coefficient μ

From equation (14): $\mu = \dfrac{k}{\omega_r Q}$ gm cm^2/sec

$\mu = 1.09 \times 10^4$ gm cm^2/sec

IV. Moment of Inertia of Transducer Head plus Virtual Water Mass

From equation (10): $I_1 = \dfrac{\mu}{2\pi \, (B.W.)}$ gm cm^2

$I_1 = 869$ gm cm^2

V. Moment of Inertia of Transducer Head

From equation (3): $I_2 = \dfrac{k}{\omega_r^2}$

where ω_r is the resonant frequency in air.

$I_2 = 630$ gm cm^2

VI. Moment of Inertia of Virtual Water Mass

$I_3 = I_1 - I_2$

$I_3 = 239$ gm cm^2

VII. Transducer Sensitivity

From equation (3): $\dfrac{\Delta\omega}{\omega} = \dfrac{1}{2} \dfrac{\Delta I_1}{I_1}$

or $\dfrac{\Delta\omega}{\omega} = \dfrac{1}{2} \dfrac{\Delta I_3}{I_2 + I_3} = \dfrac{1}{2} \dfrac{\Delta I_3}{I_3} \left(\dfrac{1}{1 + \dfrac{I_2}{I_3}}\right)$

$= \dfrac{1}{2} \dfrac{\Delta I_3}{I_3} \left(\dfrac{1}{1 + 2.64}\right)$

But because $I_3 \sim \rho$,

$\dfrac{\Delta\omega}{\omega} = \dfrac{\Delta\rho}{\rho} \dfrac{1}{7.3}$

VIII. Torque Generated

From equation (27): $\tau = (BINS)(10^7)$ dyne cm

$\tau = 1.68 \times 10^4$ dyne cm

IX. Angular Displacement Amplitude

from equation (26): $\hat{\theta} = \dfrac{Q\tau}{k}$ radians

$\hat{\theta} = .51 \times 10^{-3}$ radians

X. Energy Dissipation in Torsion Coil

$$P = \left(\frac{I}{\sqrt{2}}\right)^2 R$$

$$P \simeq 0.22 \text{ watts}$$

XI. Frequency Error Caused by Damping Coefficient μ

The maximum instantaneous zero crossing error is

$\Delta\alpha$ max. inst. $= 10^{-3}$ cycles $= 2\pi \times 10^{-3}$ radians. When averaged

over n cycles, the average zero crossing error is $\overline{\Delta\alpha} = \dfrac{\Delta\alpha \text{ max. inst.}}{n}$.

Typical averaging time of 2 seconds gives $n \simeq 1,000$. Thus

$\overline{\Delta\alpha} = 2\pi \times 10^{-6}$ radians.

From equation (24):

$$\frac{\dfrac{\Delta\omega}{\omega}}{\dfrac{\Delta\mu}{\mu}} = \frac{\overline{\Delta\alpha}}{2Q} = \frac{2\pi \times 10^{-6}}{(2)(239)} = 1.3 \times 10^{-8}$$

XII. Temperature Coefficient of Resonant Frequency

From equation (29): $\dfrac{1}{\omega_r}\dfrac{d\omega_r}{dT} = \dfrac{1}{2}\left[\dfrac{1}{k}\dfrac{dk}{dT} - 5\alpha_T\right]$

$\frac{1}{k} \frac{dk}{dT}$ is not well known for the material used in this prototype.

Assuming the worst case, and using

$$\frac{1}{k} \frac{dk}{dT} = -30 \times 10^{-6}/°C$$

$$\alpha_T = 16 \times 10^{-6}/°C$$

gives $\quad \frac{1}{\omega_r} \frac{d\omega_r}{dT} = -55 \times 10^{-6}/°C$

XIII. Maximum Velocity of Transducer Vanes

Angular displacement θ is given by

$$\theta = A \sin \omega_r t \quad \text{where } A = .5 \times 10^{-3} \text{ radians}$$

The peak velocity $\hat{v}$ of the vanes at the outer radius R is:

$$\hat{v} = \left| \frac{d\theta}{dt} R \right| = A\omega_r R$$

$$\hat{v} = 6 \text{ cm/sec}$$

TABLE II

Specifications

I. Transducer Head

    a) Material: #304 stainless steel

    b) Dimensions: as per Figure VI

    c) Thermal Expansion Coefficient: $\alpha_T = 16 \times 10^{-6}/°C$

    d) Moment of Inertia (in air): $I = 630 \text{ gm cm}^2$

    e) Moment of Inertia (including virtual mass): $I + C\rho = 869 \text{ gm cm}^2$

    f) Angular Displacement at Resonance: $.51 \times 10^{-3}$ radians

II. Torsion Bars

    a) Material: Ni-Span-C Alloy 902

    b) Dimensions: as per Figure VII

    c) Thermal Expansion Coefficient: $\alpha = 8 \times 10^{-6}/°C$

    d) Thermoelastic Coefficient: $TEC = -30 \times 10^{-6}/°C$ to $+30 \times 10^{-6}/°C$

    e) Modulus of Rigidity G: $G = 7.0 \times 10^{11} \text{ dynes/cm}^2$

    f) Torsional Spring Constant: $k = 7.8 \times 10^9 \text{ dyne cm}$

III. Strain Gages

    a) Type: Kulite Semiconductor   UGP-1000-090

    b) Resistance (each gage):   1000 Ω

    c) Gage Factor: 155

IV. Torsion Coil

    a) Material: #40 AWG enamel insulated magnet wire

    b) Number of Turns: 400

    c) Plotting Material: clear epoxy

    d) Peak Current: 70 ma.

    e) Resistance: 87 Ω

    f) Inductance: 3.3 mh.

V. Magnet

    a) Shape: U

    b) Field Strength: about 3,000 Gauss between the pole pieces

VI. Densitometer

    a) Sensitivity: $\dfrac{\Delta\omega}{\omega} = \dfrac{1}{7.5}\dfrac{\Delta\rho}{\rho}$

    b) Temperature Coefficient: $\sim 140 \times 10^{-6}/°C$

    c) Drift: negligible

    d) Response Time: ~ 1 second

    e) Precision: $\pm 2 \times 10^{-4}$ gms/cm^3

TABLE III

Data for Figures X & XI

Normalized Period	Density	$K_1 + K_2\rho$
1.001997	1.00473	1.00411
1.002497	1.00834	1.00506
1.002971	1.01184	1.00599
1.003074	1.01254	1.00617
1.003268	1.01395	1.00655
1.003457	1.01537	1.00692
1.003943	1.01897	1.00788
1.004426	1.02259	1.00884
1.004893	1.02614	1.00977
1.005083	1.02756	1.01015
1.005188	1.02828	1.01034
1.005377	1.02970	1.01072
1.005843	1.03330	1.01167
1.006309	1.03691	1.01263
1.006756	1.04043	1.01356
1.006945	1.04190	1.01395
1.007391	1.04550	1.01490
1.007484	1.04622	1.01509
1.007595	1.04695	1.01528
1.007692	1.04767	1.01548

TABLE IV

Data for Figure XII

Time (sec.)	Normalized Period	Time (sec.)	Normalized Period
0	1.000640	43	1.000720
	1.000640		1.000722
	1.000640	45	1.000723
	1.000640		1.000725
	1.000640		1.000726
5	1.000639		1.000726
	1.000640		1.000727
	1.000640	50	1.000728
	1.000642		1.000729
	1.000643		1.000730
10	1.000642		1.000731
	1.000643		1.000731
	1.000643	55	1.000734
	1.000642		1.000733
	1.000643		1.000733
15	1.000644		1.000733
	1.000643		1.000734
	1.000645	60	1.000734
	1.000646		1.000735
	1.000647		1.000736
20	1.000648		1.000736
	1.000651		1.000737
	1.000653	65	1.000736
	1.000658		1.000738
	1.000664		1.000737
25	1.000667		1.000738
	1.000671		1.000737
	1.000677	70	1.000737
	1.000682		1.000738
	1.000683		1.000737
30	1.000685		1.000738
	1.000692		1.000739
	1.000694	75	1.000738
	1.000698		1.000738
	1.000702		1.000738
35	1.000705		1.000738
	1.000708		1.000738
	1.000710	80	1.000739
	1.000713		1.000739
	1.000715		1.000739
40	1.000718		1.000739
	1.000718		1.000740
	1.000719		

ACKNOWLEDGMENTS

REFERENCES

Banmeister, T., ed., Mark's Standard Handbook for Mechanical Engineers, McGraw-Hill, 7th edition, 1966.

Carritt, D. E. and J. H. Carpenter, The Composition of Sea Water and the Salinity-Chlorinity Problem, in Physical and Chemical Properties of Sea Water, National Academy of Sciences-National Research Council Pub. 600, 67-86, 1958.

Cox, R. A., The Physical Properties of Sea Water, in Chemical Oceanography, Riley and Skirrow, eds., Academic Press, 73-117, 1965.

Doebelin, E. O., Measurement System: Application and Design, McGraw-Hill, New York, 743 pp., 1966.

Higdon, A., E. H. Ohlsen, and W. B. Stiles, Mechanics of Materials, John Wiley & Sons, Inc., New York, 502 pp., 1960.

Richardson, W. S., A Vibrating Rod Densitometer, in Physical and Chemical Properties of Sea Water, National Academy of Sciences-National Research Council Pub. 600, 113-117, 1958.

Washburn, E. W., ed. in chief, International Critical Tables, Vol. III, published for the National Research Council, McGraw-Hill, New York, 79, 1928.

———

Technical Bulletin T-31, Engineering Properties of Ni-Span-C Alloy 902, Huntington Alloy Products Division, International Nickel Co., Inc., 14 pp., 1963.